

## Geochemistry of Selected Hot Springs in Jiangxi Province, SE-China

Sun Zhanxue<sup>1</sup>, Chen Gongxin<sup>1</sup>, Zhang Zhichao<sup>1</sup>, E.V. Zippa<sup>2</sup> & Gao Bai<sup>1</sup>

1-State Key Laboratory of Nuclear Resources and Environment, East China University of Technology, Nanchang, Jiangxi, China

[zhxsun@ecut.edu.cn](mailto:zhxsun@ecut.edu.cn)

2- National Research Tomsk Polytechnic University, 634050, Tomsk, Lenina st. 30, Russia

zev-92@mail.ru

**Keywords:** nitric hot springs; carbon dioxide-dominated hot springs; hydrogeochemistry; isotopes; water-rock interaction; China.

### ABSTRACT

The chemical and isotopic composition of ten selected hot springs in Jiangxi Province, SE-China, are analyzed. Five of them are N<sub>2</sub>-dominated hot springs. The N<sub>2</sub>-dominated geothermal waters are characterized by low TDS ranging from 0.135g/L to 0.294g/L, high pH values (>8.5), and nitrogen-predominate (>90%) in dissolved gases. The rest are CO<sub>2</sub>-dominated hot springs. The CO<sub>2</sub>-dominated thermal waters are distinguished by higher salinity from 0.245g/L to 1.33g/L but lower pH values (<8.0) and carbon dioxide-dominated (>96%) in dissolved gases. Fluid-mineral equilibrium studies suggest that the geothermal water-rock system is an equilibrium -nonequilibrium system in which geothermal waters are close to equilibrium with secondary minerals as carbonates and fluoride, but disequilibrium with endogenous minerals as albite and anorthite. The reasons for extremely low TDS of the nitric hot springs is also discussed based on geochemical modeling using geochemical code PHREEQC. Solute geothermometers and the Log(Q/K) method give subsurface temperatures ranging on average from 80 to 150°C for the nitric geothermal systems. The isotopic studies showed that the nitric hot springs were recharged by local precipitation and have a circulation depth approximately from 1200m to 2700m. Isotopic and gas study showed that the carbon dioxide of the CO<sub>2</sub>-dominated hot springs are originated from magmatic inorganic sources and the nitrogen of the type is the mixture of mantle derived, crustal and atmospheric N<sub>2</sub>, and that the CO<sub>2</sub> for the N<sub>2</sub>-dominant type come from crustal organic sources and the <sup>3</sup>He/<sup>4</sup>He ratios represents input of radiogenic <sup>4</sup>He in the crust.

### 1. INTRODUCTION

Jiangxi Province, located in SE-China, is one of the Provinces in the country with a wide distribution of hot springs. There are over 118 hot springs that have been found in the Province. The hot springs are mainly distributed along NNE and EW-trending uplift belts and controlled by the NNE and NE-trending faults.

The temperatures of most hot springs in the Province are lower than 90 °C. The highest temperature of them is 88 °C of the Tanghu Hot spring, located in the southern part of the Province. Most of the hot springs in Jiangxi Province belongs to medium and low temperature geothermal water (table1). There are two types of hot springs in the Province: one is the nitric geothermal water and the other is the carbon dioxide-dominated geothermal water (Sun et al., 2014). The nitric thermal waters has lower TDS of 0.2–0.6 g/L but higher pH values (>8.5), and the carbonate dioxide geothermal has higher TDS of 0.5–3.0 g/L but lower pH values (<7.6). The formation mechanisms of the geothermal waters in the Province are not very clear.

**Table 1: Temperatures of hot springs in Jiangxi province**

Temperature(°C)	20-40	40-60	60-80	>80
Numbers	66	36	13	3
Percentage (%)	56	30.5	11	2.5

Geochemistry plays a very important role in providing useful information on the origin of the geothermal fluids, the occurrence of mixing processes among different components, the role of water–rock and water–gas interactions, and the flow regimes (Ármansson H., 1989; Arnórsson S., 2000). This paper presents the formation mechanism of the nitric thermal waters in the Province by using geochemical data including water chemistry and isotopic analyses.

### 2. SAMPLING AND ANALYTICAL METHODS

This paper presents the results of 10 samples of hot springs collected. Temperature, pH, conductivity and redox potential were analyzed using Multi-function parameter 520M-01A in the field. The values of dissolved oxygen for the hot springs were analyzed using a dissolved oxygen meter, and the dissolved SiO<sub>2</sub> (Method 8185) and Fe concentrations (Method 8147) were determined by HACH DR2400 portable spectrophotometer on site. HCO<sub>3</sub><sup>-</sup> and CO<sub>3</sub><sup>2-</sup> were titrated with 10 ml micro-titrate tube. Major anions were analyzed by Ion ICS-1100 chromatography such as SO<sub>4</sub><sup>2-</sup>, Cl<sup>-</sup>, F<sup>-</sup>, NO<sub>3</sub><sup>-</sup>, NO<sub>2</sub><sup>-</sup> and PO<sub>4</sub><sup>3-</sup>, and major cations were analyzed by iCAP7400 spectrometer such as K<sup>+</sup>, Na<sup>+</sup>, Ca<sup>2+</sup>, Mg<sup>2+</sup>, Fe, and Cu. Ten samples were analyzed for D and <sup>18</sup>O at the State Key Laboratory of Nuclear Resources and Environment of East China University of Technology. A Finnigan MAT253 mass spectrometer was used for the measurements. Samples of δD were equilibrated with mixture gas of 2% H<sub>2</sub> and He at a temperature of 45 °C for 40 minutes and then detected by MAT253, resulting in accuracy less than 2 ‰. Samples of δ<sup>18</sup>O were equilibrated with a mixture gas of 0.3% CO<sub>2</sub> and He at a constant temperature of 28 °C for 20 hours resulting in accuracy less than 0.2‰. The samples were standardized using in-house standards of known composition relative to V-SMOW (Standard Mean Ocean Water).

### 3. RESULTS AND DISCUSSION

#### 3.1 Chemical characteristics

Chemical analysis were as shown in Table 2, the charge balance error of all samples was less than 5%.

**Table 2: Results of chemical analysis of hot springs (mg/L)**

Sample NO.	K <sup>+</sup>	Na <sup>+</sup>	Ca <sup>2+</sup>	Mg <sup>2+</sup>	Cl <sup>-</sup>	SO <sub>4</sub> <sup>2-</sup>	HCO <sub>3</sub> <sup>-</sup>	CO <sub>3</sub> <sup>2-</sup>	F <sup>-</sup>
1	93.3	126	121	11.8	10.8	42.6	673	/	4.41
2	15.2	10.9	57.1	2.89	2.05	50.1	140	/	4.5
3	19.5	221	37.6	0.15	16.9	451	31.5	/	8.51
4	59.2	703	86	4.98	28.9	257	1820	/	5.96
5	3.68	69.8	11.8	0.06	7.13	25.7	131	/	10.6
6	8.3	89.3	22.6	0.47	5.01	25.3	250	/	9.03
7	1.98	71.9	3.76	0.02	6.16	17.3	126.7	3.24	13.7
8	4.49	59.1	7.5	0.14	3.91	37.4	94.06	6.94	8.55
9	5.09	71.6	6.19	0.03	4.33	13.2	131.1	6.94	13.3
10	3.06	66.1	2.34	0.03	6.03	23.9	67.3	16.2	13.2

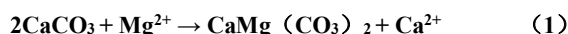
  

Sample NO.	TDS (mg/L)	T(°C)	pH	SiO <sub>2</sub>	Hydrochemical type
1	651	35.8	6.3	73.5	HCO <sub>3</sub> -Ca-Na
2	187	52.8	7.93	45	HCO <sub>3</sub> -SO <sub>4</sub> -Ca
3	568	58.1	6.86	107.1	SO <sub>4</sub> -Na
4	1330	52.2	6.87	117	HCO <sub>3</sub> -Na
5	245	72.0	7.72	76.1	HCO <sub>3</sub> -Na
6	294	42.3	8.88	91	HCO <sub>3</sub> -Na
7	173	37.8	8.82	61.8	HCO <sub>3</sub> -Na
8	129	83.0	8.75	122	HCO <sub>3</sub> -SO <sub>4</sub> -Na
9	135	82.3	8.30	96	HCO <sub>3</sub> -Na
10	135	41.4	9.23	104	HCO <sub>3</sub> -Na

As shown in Table 2, the TDS values of the nitric hot springs (No. 6, 7, 8, 9, 10) are lower than those of the carbon dioxide type hot springs (No. 1, 2, 3, 4, 5). The Piper diagram (Figure 1) shows that most of the nitric hot springs are the HCO<sub>3</sub>-Na type waters with lower TDS.

The average value of the  $\gamma_{Na/\gamma_{Cl}}$  coefficient of the seawater is 0.85. If the groundwater is mainly dissolved from the rock salt, the  $\gamma_{Na/\gamma_{Cl}}$  ratio is close to 1. The  $\gamma_{Na/\gamma_{Cl}}$  ratios of nitric hot springs in Longnan area of the Province are much greater than 1, indicating that the hot springs have undergone strong water-rock interactions. In the magmatic and metamorphic rocks, the host rocks of thermal reservoirs contain lots of carbonates and aluminosilicate minerals, which were leached by CO<sub>2</sub> and H<sub>2</sub>O. Those minerals such as feldspar are hydrolyzed to produce Na<sup>+</sup>, and the aluminosilicate minerals are weathered and dissolved to form low TDS water mainly composed of HCO<sub>3</sub><sup>-</sup> and Na<sup>+</sup>.

The low content of K<sup>+</sup> and Mg<sup>2+</sup> in hot spring may be due to K<sup>+</sup> and Mg<sup>2+</sup> which are easily absorbed by plants. In addition, K<sup>+</sup> can form secondary minerals, such as hydromica, montmorillonite, sericite, etc., especially under the high temperature and pressure conditions, and the dolomitization may occur as the temperature increases (Equation 1), so that the hot spring is relatively lack of magnesium and rich in sodium and calcium.



Fluorine (F<sup>-</sup>) is rich in nitric hot springs, ranging from 0.45 to 0.7 meq/L, and account for more than 15% of the total of anions. This element may be derived from fluorine-contained minerals such as biotite, amphibole and fluoroapatite in magmatic rocks.

The pH values of the nitric hot spring is higher than those of the carbon dioxide type hot springs. Due to leaching action, the pH value in the water should gradually increase with the increasing of the minerals (especially HCO<sub>3</sub><sup>-</sup> present). For example, the hydrolysis of albite, the common mineral in the rocks of this area, results in increasing of OH<sup>-</sup> in waters (see Equation 2).



According to research by Shvartsev (Shvartsev, 2015), the alkalinity produced by the hydrolysis of silicate minerals is neutralized to some extent by acids (inorganic or organic acids) in geothermal systems. In the nitric hot springs of the Baikal region, it is difficult to produce large amounts of H<sub>2</sub>CO<sub>3</sub> and CO<sub>2</sub> substances due to the scarcity of humus and organic matter in cold and barren landforms. Therefore, in the case where the carbon dioxide gas is extremely scarce, pH of the solution increase as the increasing of alkaline substances.

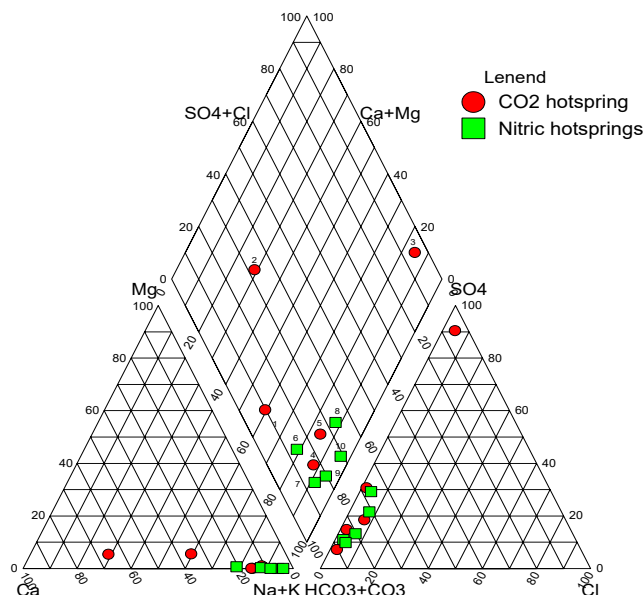


Figure1: Piper diagram of hot springs

### 3.2 Hydrogen and oxygen isotope characteristics

Craig (1961) first proposed that the precipitation points around the world fall on the line of  $\delta D = 8\delta^{18}O + 10$ . Further research has shown that the slope and intercept of atmospheric precipitation may vary within a small range, depending on the origin of water vapor that forms the precipitation process and other meteorological factors. The slope and intercept of the atmospheric precipitation line can be used to identify the recharge of groundwater. In this region, the local atmospheric meteoric water of Jiangxi province is (Sun et al., 2001):

$$\delta D = 8.4\delta^{18}O + 11.8 \quad (3)$$

For the hot springs in southern Jiangxi Province,  $\delta^{18}O$  have shifted obviously (as shown in Figure.2), indicating that water-rock interactions are quite strong in the geothermal systems.

In the southwestern part of China, the altitude gradient of  $\delta D$  is  $-2.5\text{‰}/100\text{m}$  which is lower than that in the southwest with the elevation gradient of  $-2\text{‰}/100\text{m}$  (Sun Z. & Li L., 2001). According to the isotopic altitude effect, the recharge altitude of geothermal waters can be calculated using Equation 4.

$$H = \frac{R - R_1}{\rho} + h \quad (4)$$

where, H is the recharge altitude of the geothermal water, R is the  $\delta^{18}O$  or  $\delta D$  value of the hot spring,  $R_1$  is the  $\delta^{18}O$  or  $\delta D$  value of the surface water without obvious evaporation near the sampling point, h is the surface water elevation,  $\rho$  is the altitude gradient of  $\delta^{18}O$  or  $\delta D$ . Due to obvious oxygen-shift of the selected geothermal waters in the Province, the recharge altitude of the thermal waters can only be estimated by Equation 4 using altitude gradient of  $\delta D$  and the results are shown in Table 3.

Table 3: calculated Results for recharge altitude of hot springs

Hot spring No.	Sampling Altitude /m	$\delta D/\text{‰}$	Recharge Altitude/m
1	75	-53.1	230
2	62	-55.0	312
3	186	-59.0	636
4	228	-55.9	523
5	310	-60.6	840
6	290	-61.0	840
7	369	-57.8	759
8	341	-59.6	821
9	311	-66.2	1121
10	276	-66.6	1106

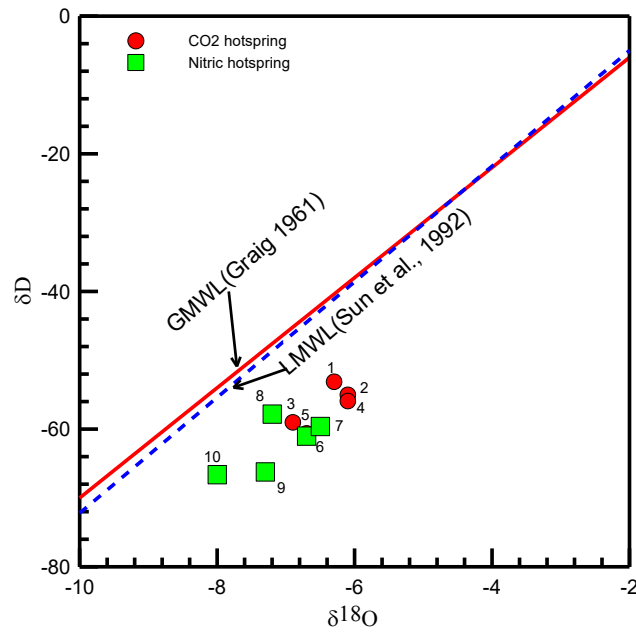


**Figure 2: Relationship between  $\delta D$  and  $\delta^{18}O$  of nitric hot springs**

### 3.3 Fluid-mineral equilibrium

The saturation index (SI) is one of the most widely used hydrogeochemical parameters in groundwater research. When the mineral is in equilibrium in aqueous solution,  $SI = 0$ ; when the mineral dissolves,  $SI < 0$ ; when the mineral precipitates,  $SI > 0$ . The definition of saturation index (SI) can be expressed as Equation 5

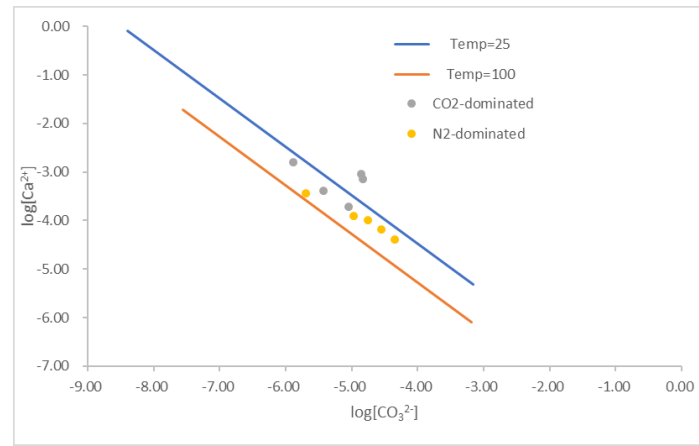
$$SI = \log IAP/K \quad (5)$$

where, IAP is ion activity product and K is the equilibrium constant. This equation is established at 25 ° C and 100 ° C. Here, PHREEQC2.15 was used to calculate the saturation indexes of some secondary minerals of the 5 nitric hot springs. The calculation results are shown in table 4.

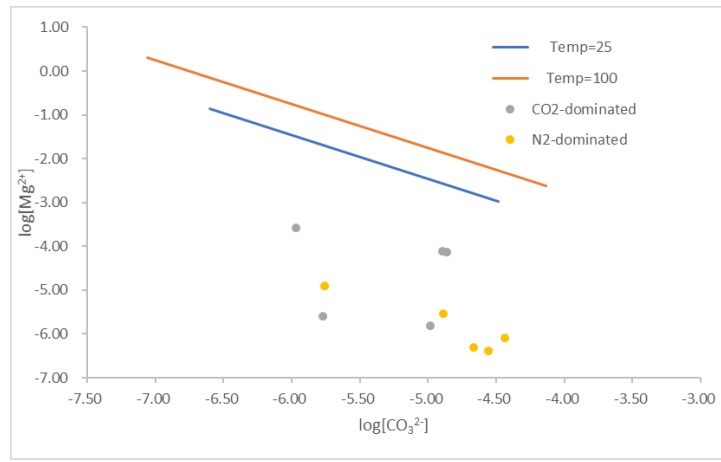
**Table 4: Saturation indexes of secondary minerals in nitric hot springs**

Sample NO.	Albite	Calcite	Chalcedony	Dolomite	Fluorite	Siderite	Quartz	Magnesite
6	-1.05	-0.53	0.29	-2.26	0.26	-2.32	0.67	-1.61
7	-5.79	-0.15	-1.19	-2.32	-0.06	-2.77	-0.80	-3.1
8	-4.08	0.30	-0.54	-0.99	-0.49	-1.71	-0.27	-2.62
9	-4.91	0.34	-0.80	-1.58	-0.19	-2.35	-0.52	-2.93
10	-2.48	0.09	-0.29	-1.26	-0.36	-1.95	0.088	-1.23

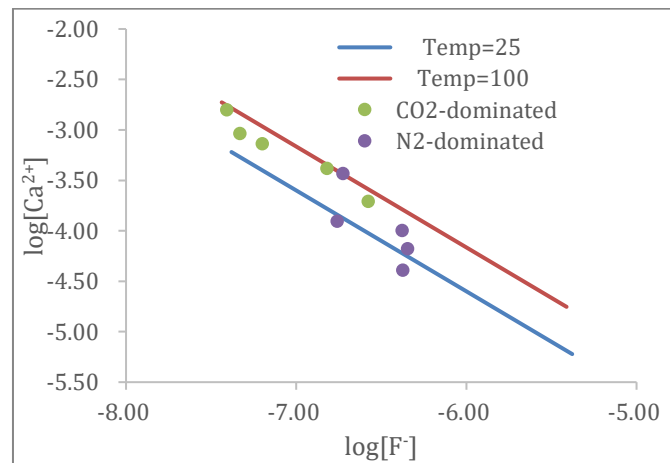
Figure 4 shows the saturated state of carbonate mineral calcite ( $CaCO_3$ ), magnesite ( $MgCO_3$ ) and fluorite ( $CaF_2$ ). Figure 4 showed that the calcite minerals reach an equilibrium state, and magnesite is obviously below the line at  $SI=0$ , being in an undersaturated state. Since the solubility of carbonate decreases with increasing temperature, the equilibrium level of hot spring and carbonate minerals increases with depth. Fluorite ( $CaF_2$ ) is another mineral that can reach saturation under moderate temperature parameters (Fig. 4c). It can be seen from the Figure 4 that the fluorite in the hot springs is mostly in equilibrium with the solution. Like calcite, fluorite in hot springs can reach saturation in the case of low salinity ( $<0.2g/L$ ,  $pH>8$ ).



(a)



(b)



(c)

**Figure 4: Mineral equilibrium of calcite (a), magnesite (b) and fluorite (c) in hotspring at 25 ° C (dashed lines) and 100 °C (solid line))**

### 3.4 Solute geothermometers

Solute geothermometers of SiO<sub>2</sub>, chalcedony, Na-K, Na-K-Ca are widely used in geothermal studies. Mg-Na-K triangle diagram is one of the most useful geothermometers which was proposed by Giggenbach (1988).

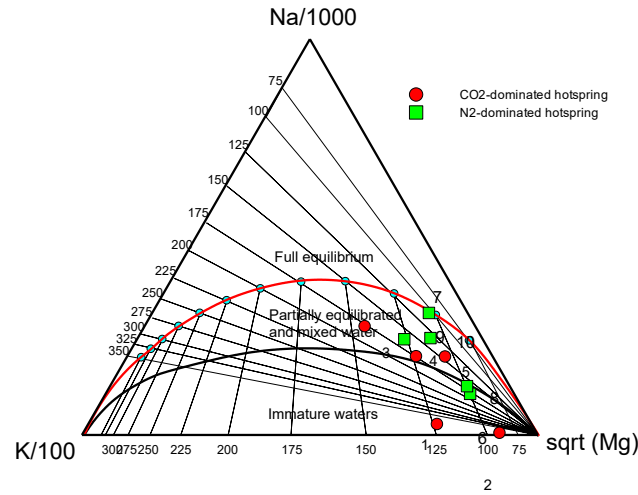


Figure 5: Na-K-Mg triangle diagram of hot springs

As shown in Figure 5, most of the nitric hot springs in the southern part of the Province are the immature waters or in partial equilibrium with relevant minerals. It is not suitable to use the cation geothermometers directly. Therefore, the chalcedony geothermometer and  $\text{SiO}_2$  geothermometer are used to estimate the temperatures of the geothermal reservoirs. The calculation results are shown in Table 5. Temperature difference of these two geothermometers are about 20 °C. The result of chalcedony geothermometer (Equation 6) is relatively lower than those of  $\text{SiO}_2$  geothermometer (Equation 7).

Chalcedony geothermometer (Fournier,1977),  $T \in (0, 250^\circ\text{C})$

$$T = \frac{1032}{4.69 - \text{LogSiO}_2} - 273.15 \quad (6)$$

$\text{SiO}_2$  geothermometer (Fournier,1973),  $T \in (0, 250^\circ\text{C})$ ,

$$T = \frac{1309}{5.19 - \text{LogSiO}_2} - 273.15 \quad (7)$$

Table 5: Results of estimation of temperature and depth of reservoir

Sample NO.	$\text{SiO}_2$ geothermometers/ $^\circ\text{C}$	Chalcedony geothermometers/ $^\circ\text{C}$	$\text{Log}(Q/K)/^\circ\text{C}$	Reservoir depth/m
6	132	105	80—120	1833
7	112	83	120—160	1179
8	149	123	140—150	2506
9	135	108	110—130	2690
10	139	113	90—120	2117

### 3.5 $\text{Log}(Q/K)$ and T

The  $(\text{log}Q/K)$ -T diagram can be applied to estimate the subsurface temperatures of geothermal systems (Reed M. & Spycher N, 1984; Pang Z. & Reed M., 1998). The  $(\text{log}Q/K)$ -T diagram of the Rucheng Hot spring (No.8) of the western part of the Province showed that sepiolite, quartz and chalcedony converge at about 140-150°C. The temperature of the reservoir in Rucheng Hotspring may be estimated as 140-150 °C.

As shown in Figure 6(b), the calcite and chalcedony converge at 83 °C, and quartz at 118 °C. Therefore, the temperature of reservoir for Hetong Hotspring (No.6) is in the range of 80 °C to 120 °C. As shown in Figure 6(c), silica, chalcedony and aragonite are converged at 120 °C, 140 °C and 150 °C, respectively. Therefore, the temperature of reservoir for Dayu Hotspring (No.7) may be in the range of 120 °C to 150 °C. As shown in Figure 6 (d), forsterite and sepiolite are converged at around 110-130 °C. Therefore, the temperature of reservoir in Tanghu Hotspring (No.9) may be estimated as 110-130 °C. In figure 6(e), six minerals such as quartz, chalcedony, sepiolite, calcite, aragonite and clinoenstatite converge at 90-120 °C. Therefore, the subsurface temperature for Zhangmu Hotspring (No. 10) may range from 90 to 120 °C.

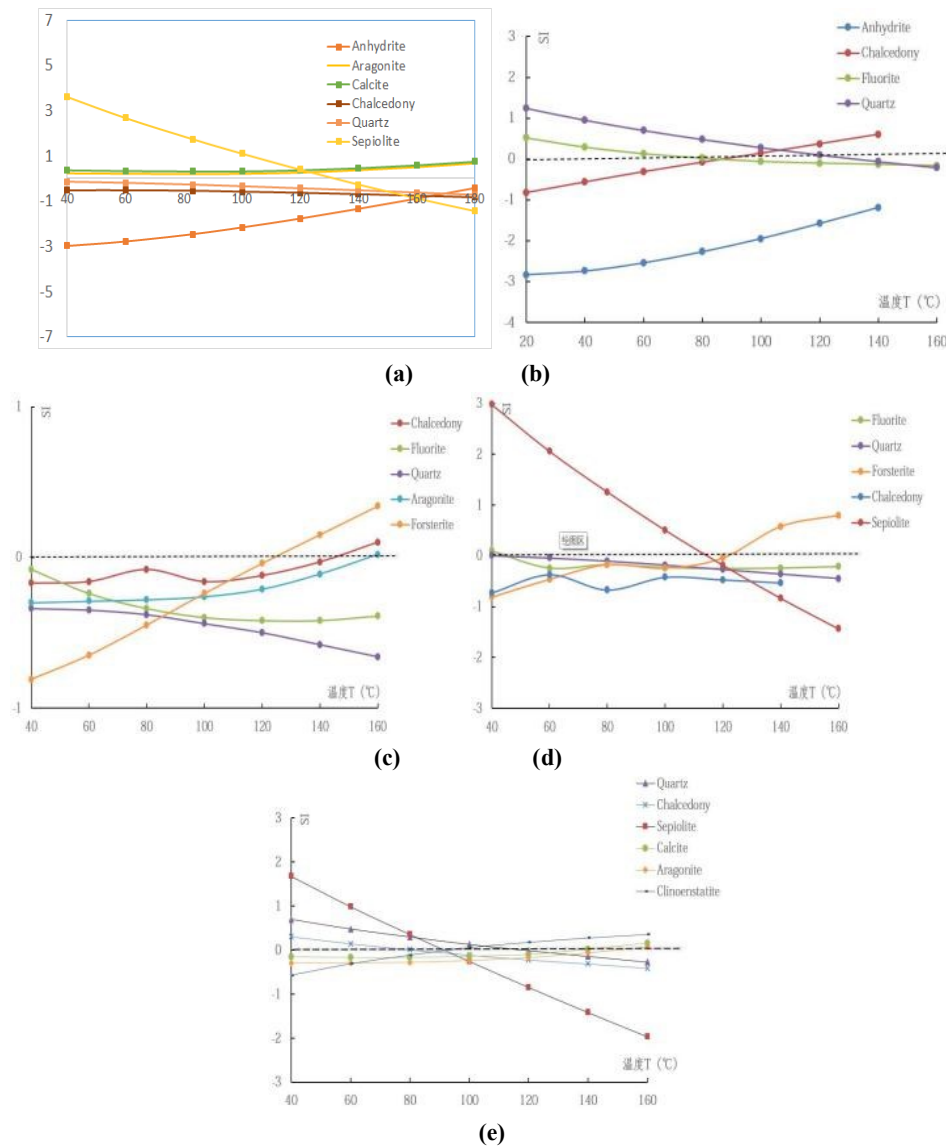


**Figure 6: logQ/K of Hot springs (a: Rucheng Hot Spring; b: Hetong Hot Spring; c: Dayu Hot Spring; d: Tanghu Hot Spring; e: Zhangmu Hot Spring)**

### 3.6 Circulation depth

The isothermal zone is generally 15-20 m depth in the Province. The annual temperature change at this depth is less than 0.1 °C. Circulation depth of the hot spring is calculated by the following formula:

$$t = (D-h) \frac{\Delta t}{\Delta Z} + t_0 \quad (8)$$

where:  $t$ —subsurface temperature of geothermal reservoir ( $^{\circ}\text{C}$ );

$D$ —Circulation depth (m);

$H$ —depth of isothermal zone (m);

$\frac{\Delta t}{\Delta Z}$ —Geothermal gradient ( $^{\circ}\text{C}/\text{m}$ );

$t_0$ —local annual average temperature or normal temperature ( $^{\circ}\text{C}$ )

In the study area, the geothermal gradient is 3.5  $^{\circ}\text{C}/100\text{ m}$  (Hu Shengbiao et al., 1992),  $t_0$  is the annual average ground temperature of the recharge area (22  $^{\circ}\text{C}$ ), and the  $H$  is taken as 20 m. The results of estimated circulation depth for the hot springs are shown in Table 5.

### 3.7 Isotopic and geochemical evidence for origin of geothermal gases

#### 3.7.1 Carbon isotopic composition and genesis of $\text{CO}_2$ and $\text{CH}_4$ in geothermal gas

The  $\delta^{13}\text{C}$  of nitrogen-type geothermal gas in the western region of southern Jiangxi is -23.7‰ ~ -12.6‰ (PDB), and the average value is -17.82‰. According to the identification of  $\text{CO}_2$  genesis (Dai Jinjin et al., 1994), this  $\text{CO}_2$  gas is an organic factor of crustal origin. The  $\delta^{13}\text{C}$  values of  $\text{CO}_2$  for the  $\text{CO}_2$ -dominant type geothermal gases are -5.50‰ to -3.49‰ (PDB) with a mean value of -4.66‰ (PDB) showing that the carbon dioxide of the gases are originated from magmatic inorganic sources.

### 3.7.2 Noble gases and isotopes in geothermal gases

Geothermal fluids may contain helium from the mantle, crust, or atmosphere. Helium of different origins has characteristics of helium isotope composition, so it can be distinguished from different origin by the contribution of helium to geothermal fluid. The  $^3\text{He}/^4\text{He}$  ratios of the  $\text{N}_2$  dominant gases are from 0.06 to 0.13  $R_a$ , representing input of radiogenic  $^4\text{He}$  in the crust. The  $^4\text{He}/^{20}\text{Ne}$  and  $^3\text{He}/^4\text{He}$  demonstrate that the  $\text{N}_2$  dominant gases are of atmospheric origin with some crustal contributions.

The  $^3\text{He}/^4\text{He}$  ratio of carbon dioxide hot spring gas in the southeast of the Province ranges from  $1.90 \times 10^{-6}$  to  $3.18 \times 10^{-6}$ , and  $R/R_a$  from 1.36 to 2.27, all of which are greater than 1 (Sun Z. et al., 2014). Firstly, considering the origin of crust and mantle sources, 0.02  $R_a$  and 8  $R_a$  were taken as the  $^3\text{He}/^4\text{He}$  of typical crust and mantle sources, and the proportion of mantle source helium in geothermal gas could be estimated by using the binary mixing model (Du J, 1994):

$$A = \frac{(R_s - R_c)}{(R_m - R_c)} \times 100\% \quad (9)$$

where, A is the proportion of mantle source helium in natural gas, and  $R_s$ ,  $R_c$  and  $R_m$  represent the  $^3\text{He}/^4\text{He}$  values of samples, crustal sources and mantle sources, respectively. As  $R_s$  value is 1.36  $R_a$  and 2.27  $R_a$  respectively, it can be concluded from formula (1) that the proportion of hot spring mantle source helium in the total helium in this area is in the range of 16.8% to 28.2%. If the geothermal gas in this area is mainly derived from mantle source and air source, the proportion of mantle source helium in total helium is 5.1% ~ 18.1% with this calculation. In addition, it may be the mixing of crustal origin, mantle source and air. It indicates that the helium in the hot spring gas in the southeastern Jiangxi Province has different origin of mantle source. Results indicate that up to 28.2% of the total helium is derived from the mantle.

In this study, the  $^3\text{He}/^4\text{He}$  -  $^4\text{He}/^{20}\text{Ne}$  relationship of 6 samples collected from southern Jiangxi, as shown in figure 2. For comparison, data from Tengchong hot spring in yunnan (wang xianbin et al., 1993) are also shown in figure 2. The  $^4\text{He}/^{20}\text{Ne}$  ratio of nitrogen-type geothermal hot spring gas in the western region of southern Jiangxi varies from 234 to 674. All samples falls on both sides of the line between air and crust, indicating that it is mainly caused by mixing of air and crustal gases. The hot spring gas in Tengchong volcanic area has mantle origin, air source and crustal source mixed origin, and a few spring points show mixed origin. Results indicates that the isotopic characteristics of helium and neon of nitrogen-type hot spring gas in the western region of southern Jiangxi province showing the shallow tectonic activity range in this area.

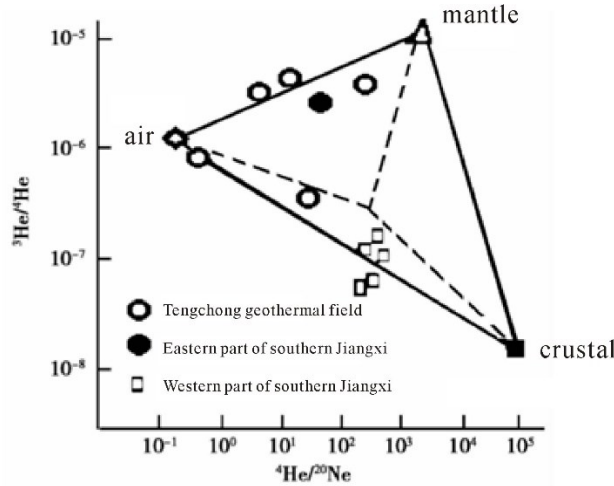


Figure 7: relation diagram of geothermal gas  $^3\text{He}/^4\text{He}$  vs  $^4\text{He}/^{20}\text{Ne}$  in southern Jiangxi province

Only one of  $\text{CO}_2$  geothermal gas in southeast Jiangxi with the data of  $^3\text{He}/^4\text{He}$  vs  $^4\text{He}/^{20}\text{Ne}$ , falls in the mixing zone of crust, mantle and air, indicating that it is mainly the mixing origin of mantle source and air, and the contribution of crustal source.

### 3.7.3 The relative content of $\text{N}_2$ -He-Ar in geothermal gas

There are four types of  $\text{N}_2$  sources in natural gas, atmospheric, biological, magma, and mantle sources. The relative composition of He, Ar and  $\text{N}_2$  in gas were used to distinguish the different origins of geothermal and volcanic gases (Giggenbach, 1992; Zhao Ping, 1992). The  $\text{N}_2/\text{Ar}$  ratio in the atmosphere is 84, and the  $\text{Ar}/\text{He}$  ratio is close to 1800. The ratio of  $\text{N}_2/\text{He}$  is about 150,000. The atmospheric precipitation  $\text{N}_2/\text{Ar}$  ratio is about 38 with  $\text{Ar}/\text{He}$  ratio 6800, and the  $\text{N}_2/\text{He}$  260,000. The gas released from the plate collision zone, Anshan magma has a high  $\text{N}_2/\text{Ar}$  values (2500 ~ 5000) and high  $\text{N}_2/\text{He}$  values (1700 ~ 5000).  $\text{N}_2/\text{He}$  values of basaltic magma and crustal source gases are 10 ~ 220.

The relative contents of He, Ar and  $\text{N}_2$  of geothermal gas in southern Jiangxi were plotted on the He-Ar- $\text{N}_2$  map of Giggenbach (1992) (Figure 3). Hot spring gas in western of Jiangxi is mainly distributed in the mixing area of atmosphere and crustal origin, which is a shallow heat storage area. Its  $\text{N}_2/\text{Ar}$  value varies from 56.15 to 83.60, indicating that  $\text{N}_2$  is mainly atmospheric origin. As mentioned above, in the west of Jiangxi geothermal gases helium isotope ratio ( $R/R_a$ ) change in between 0.06 ~ 0.13, showing obvious crustal origin radiation causes He join, this is the ratio of  $\text{N}_2/\text{He}$  (in 116.44 ~ 388.56) is far lower than atmospheric  $\text{N}_2/\text{He}$  ratio (150000) and the  $\text{Ar}/\text{He}$  than (in 1.39 ~ 6.92) also is lower than atmospheric  $\text{Ar}/\text{He}$  ratio (1800). It can be seen that  $\text{N}_2$  in the hot spring gases in the west of the Province mainly comes from the atmosphere, and may be added with crustal origin  $\text{N}_2$ .



Samples in the southeastern part of Jiangxi Province fall into the deep thermal area, and their  $N_2/Ar$ ,  $N_2/He$ , and  $Ar/H$  ratios are 9.53 to 20.11, 84.94 to 139.42, respectively. Relative He, Ar and  $N_2$  contents reveal that the nitrogen of the type of gases is the mixture of mantle derived, crustal and atmospheric  $N_2$ .

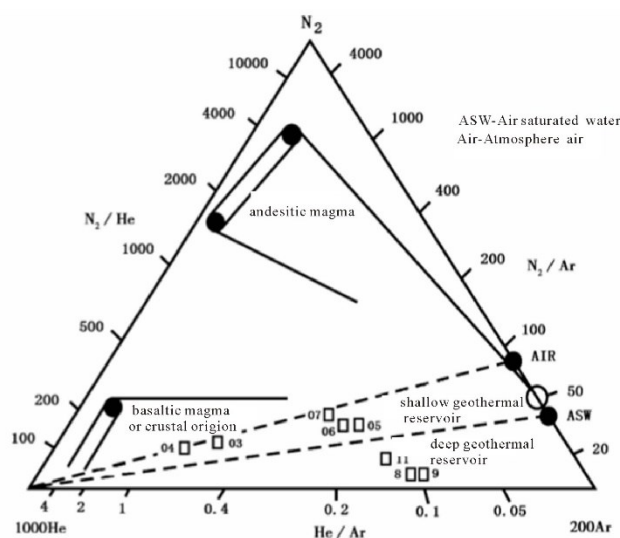


Figure 8: Relative  $N_2$ , He and Ar contents

#### 4. CONCLUSIONS

1. The  $N_2$ -dominated geothermal waters in Jiangxi Province are characterized by low TDS ranging from 0.135g/L to 0.294g/L, high pH values ( $>8.5$ ), and nitrogen-predominate ( $>90\%$ ) in dissolved gases. The  $CO_2$ -dominated hot springs in the Province are distinguished by higher salinity from 0.245g/L to 1.33g/L but lower pH values ( $<8.0$ ) and carbon dioxide-dominated ( $>96\%$ ) in dissolved gases.
2. Fluid-mineral equilibrium studies suggest that the geothermal waters are close to equilibrium with secondary minerals as carbonates and fluoride, but disequilibrium with endogenous minerals such as albite and anorthite. Solute geothermometers and the  $\log(Q/K)$  against temperature method give subsurface temperatures ranging on average from 80 to  $150^\circ\text{C}$  for reservoir hosting the nitric waters.
3. The isotopic studies show that the nitric hot springs were recharged by local precipitation and have a circulation depth approximately from 1200m to 2700m. The carbon dioxide of the  $CO_2$ -dominated hot springs are originated from magmatic inorganic sources and the nitrogen of the geothermal gases is the mixture of mantle derived, crustal and atmospheric  $N_2$ , and the  $CO_2$  for the  $N_2$ -dominant type come from crustal organic sources, and the  $^3\text{He}/^4\text{He}$  ratios represents input of radiogenic  $^4\text{He}$  in the crust.

#### REFERENCES

- Ármannsson H., Predicting calcite deposition in Krafla boreholes [J]. *Geothermics*, 1989, 18: 25-32.
- Arnórsson S. Isotopic and geochemical techniques in geothermal exploration, development and use[R]. International Atomic Energy Agency, 2000, pp. 351.
- Fournier R.O., Truesdell A.H. An empirical Na-K-Ca geothermometer for natural waters[J]. *Geochim Cosmochim Acta*, 1973, 37: 1255-1275.
- Fournier R.O., Chemical geothermometers and mixing models for geothermal systems[J]. *Geothermics*. 1977, 5: 41-55.
- Giggenbach W. F.. Geothermal solute equilibria. derivation of Na-K-Mg-Ca geoindicators[J]. *Geochimica et cosmochimica acta*, 1988, 52(12): 2749-2765.
- Pang Zhonghe, and Reed, M. Theoretical chemical thermometry on geothermal waters: Problems and methods. *Geochim. Cosmochim. Acta*, 1998, 62:1083-1091.
- Reed M., Spycher N. Calculation of pH and mineral equilibria in hydrothermal waters with application to geothermometry and studies of boiling and dilution. *Geochim. Cosmochim. Acta*, 1984, 48: 1479-1492.
- Shvartsev S.L., Zamana L.V., Plyusnin A.M., et al. Equilibrium of nitrogen-rich springs waters of the Baikal rift zone with host rock minerals as a basis for determining mechanisms of their formatio. *Geochemistry International*. 2015, Vol, 53, No. 8, pp. 713-725.
- Sun ZX, Li XL. Studies of geothermal waters in Jiangxi Province using isotope techniques. *Science in China (Series E)* 2001; 44s: 144-150.

Sun et al.

Sun Z., Bai G. and Zhanshi Z. Isotopic and geochemical evidence for origin of geothermal gases from hotspots in southern Jiangxi Province, SE China. Chinese Journal of Geology, 2014: 49(3):791-798.

Zhao Ping. Chemical thermodynamic equilibrium of gas-water-rock system in geothermal system and its simulation calculation[J].Acta Petrologica Sinica,1992,8(4):311-323.